J Musculoskel Neuron Interact 2000; 1:45-51

Original Article

Hylonome

Micro CT and Micro MR imaging of 3D architecture of animal skeleton

Y. Jiang, J. Zhao, D.L. White, H.K. Genant

Osteoporosis and Arthritis Research Group, Department of Radiology, University of California, San Francisco, USA

Abstract

Quantitative assessment of three-dimensional (3D) trabecular structural characteristics may improve our ability to understand the pathophysiology of osteoporosis, to test the efficacy of pharmaceutical intervention, and to estimate bone biomechanical properties. Considerable progress has been made in advanced imaging techniques for noninvasive and/or nondestructive assessment of 3D trabecular structure and connectivity. Micro computed tomography (μCT) has been used to measure 3D trabecular bone structure in rats, both in vivo and in vitro. It can directly quantify 3D trabecular bone structure such as trabecular volume, trabecular thickness, number, separation, structure model index, degree of anisotropy, and connectivity, in a model-independent manner. We have used μCT to study ovariectomy (OVX) induced osteopenia in rats and its treatment with agents such as estrogen, and sodium fluoride. We have demonstrated that 3D μCT can quantify mouse trabecular and cortical bone structure with an isotropic resolution of 9 μm^3. It is also useful for studying osteoporosis in mice and in phenotypes of transgenic mice or gene knockout mice. μCT can be used to quantify osteogenesis in mouse Ilizarov leg lengthening procedures, to quantify osteoconduction in a rat cranial defect model, and to quantify cortical bone porosity. Recently, μCT using high intensity and tight collimation synchrotron radiation to achieve spatial resolution of 1-2 μm has provided the capability to assess additional features such as resorption cavities. Unlike μCT, micro magnetic resonance imaging (μMRI) is nonionizing. Recently, the ability of μMRI to assess osteoporosis in animal models has been explored. Using a small, high-efficiency coil in a high-field imager, μMRI can give resolutions sufficient to discriminate individual trabeculae. We have shown that, with appropriate settings, it is possible to image trabecular bone in rats in vivo and in vitro. In our study of OVX rats, analysis of μMR images can demonstrate differences in rat trabecular bone that are not detected by DXA measurements. In a rabbit OA model, with the OA induced by meniscectomy or anterior cruciate ligament transection, MRI shows decreased cartilage thickness, subchondral osteosclerosis and osteophytes, while radiographs can only show subchondral osteosclerosis and osteophytes could not be found. Advanced imaging methods are able to measure 3D trabecular structure and connectivity in arbitrary orientations in a highly automated, objective, non-user-specific manner, allowing greater numbers of samples for unbiased comparisons between controls and the disordered or treated. They can be utilized on a large sample leading to fewer sampling errors. They are non-destructive allowing multiple tests such as biomechanical testing and chemical analysis on the same sample; and non-invasive permitting longitudinal studies and reducing the number of animals needed.

Keywords: Micro CT, Micro MRI, Osteoporosis, Osteoarthritis, Osteogenesis, Animal Models

Introduction

Various non-invasive/non-destructive techniques can be used to assess osteoporotic animal models and their treatment. Conventional radiography using high detail films and small spot x-ray tubes is a noninvasive means of displaying two-dimensional (2D) animal bone structure as well as visual density. Radiogrammetry can measure cortical thickness and bone size[1]. Recently, with improvements in microfocus radiography[2], details of the bone structure of small animals can be clearly displayed, although determination of its 2D trabecular structure requires image processing. Dual x-ray absorptiometry (DXA) is widely used in preclinical studies[3]. The values measured are given as bone mineral content (BMC), or bone mineral density (BMD) that is merely a BMC corrected for the number of pixels in which it is measured. DXA is a 2D projectional

Corresponding author: Yebin Jiang, Osteoporosis and Arthritis Research Group, Department of Radiology. University of California, San Fransisco, CA 94143-0628. E-mail: Yebin.Jiang@oarg.ucsf.edu

Accepted 17 February 2000

technique, and no structural data can be derived from DXA measurements except projectional area and length. A peripheral quantitative computed tomography (pQCT) scanner specifically designed for use on animal bones has been used to determine cortical and trabecular 3D volumetric BMD and cortical bone geometry in the study of osteoporotic animal models[4]. It is difficult to determine the trabecular structure in preclinical studies because of limited spatial resolution in the pQCT images, though apparent trabecular structural parameters can be derived from pQCT images of human cubic bone specimens using special imaging processing techniques[5].

Because many studies indicate that bone strength is only partially explained by bone mineral measurements[6], quantitative assessment of trabecular structural characteristics may improve our ability to understand the pathophysiology of osteoporosis and other bone disorders, to test the efficacy of pharmaceutical intervention, and to estimate bone biomechanical properties. The mechanical competence of trabecular bone is a function of its apparent density and 3D distribution[7]. Three D structure is typically inferred indirectly from histomorphometry and stereology on a limited number of 2D sections based on parallel plate model[8]. During aging and disease such as osteoporosis, trabecular plates are perforated and connecting rods are dissolved, with a continuous shift from one structural type to the other. Thus, the traditional histomorphometric measurements that are based on a fixed model type will lead to questionable results[9]. The introduction of 3D measuring techniques in bone research makes it possible to capture the true trabecular architecture without assumptions of the structure type.

Much progress has been made in developing μCT and μMRI for noninvasive and/or nondestructive assessment of 3D trabecular structure and connectivity. The availability of 3D measuring techniques and 3D image processing methods allow direct quantification of unbiased morphometric parameters, such as direct volume and surface determination[10], model independent assessment of thickness[11] and 3D connectivity estimation[12].

μCT

The μCT system was first introduced by Feldkamp[13] who used a μfocus x-ray tube as a source, an image intensifier as a 2D detector, and a cone-beam reconstruction to create a 3D object. It was originally designed to detect small structural defects in ceramic materials. Instead of rotating the x-ray source and detectors during data collection as in clinical CT, the specimen is rotated at various angles. X-rays are partially attenuated by a specimen that is made to rotate in equal steps in a full circle about a single axis. At each rotational position, the surviving x-ray photons are detected by a planar 2D array. A 3D-reconstruction array is created directly in place of a series of 2D slices.

The 3D cone-beam μCT imaged the trabecular bone architecture in small samples of human tibias and vertebrae, ex vivo, with spatial resolution of 60 μ[13]. A resolution of 60 μ, however, although acceptable for characterizing the connectivity of human trabeculae, may be insufficient for studies in small animals like the rat, where the trabecular widths average about 50 μ and trabecular separations average 150 μ or less[14]. Furthermore, Smith and Silver[15] have reported that 3D images from cone beam scanners are inevitably distorted away from the central slice because the single-orbit cone beam geometry does not provide a complete data set. These distortions and associated loss of spatial resolution have been particularly evident in samples containing platelike structures, even when the cone beam angle is less than 6.5° [15].

The method was further enhanced by resorting to synchrotron radiation with spatial resolution of 2 μ[16], or with applications to live rats[14]. Synchrotron μCT has spatial resolutions of 2 μ because of high brightness and natural collimation of radiation sources[16]. It uses parallel beam imaging geometry, and avoids the distortions and loss of resolution inherent in cone beam methods, and has demonstrated the ability to make distortionless images of human trabecular bone using a CT at a synchrotron storage ring[16]. Recently, μCT using high intensity and tight collimation synchrotron radiation which achieves spatial resolution of 1-2 μ provides the capability to assess additional features such as resorption cavities[17].

The hardware for synchrotron radiation μCT, however, is not readily accessible. Ruegsegger et al.[18] developed a μCT device dedicated to the study of bone specimens, without requiring synchrotron radiation. Image processing

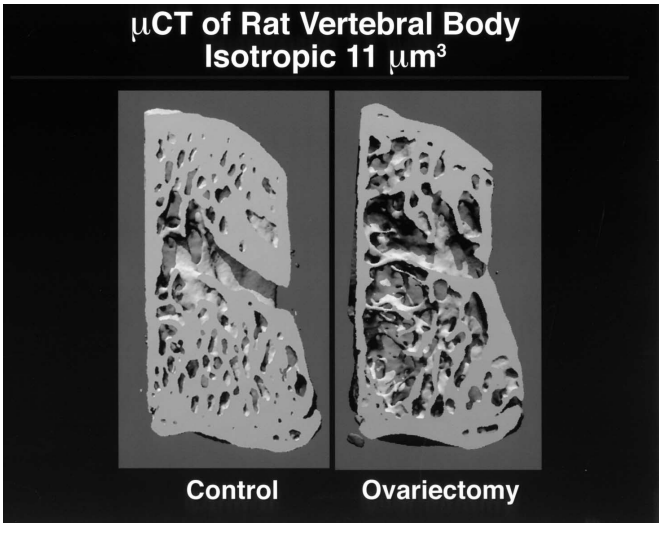

Figure 1. μCT 3D images of rat vertebral body with isotropic resolution of 11 μm^3. Compared with sham-operated control, ovariectomy results in a remarkable decrease in the trabecular bone volume, thickness, number, and a conspicuous increase in trabecular separation. The different trabecular patterns are noticeable, i.e., plate-like trabeculae in the control and rode-like trabeculae in the ovariectomized rat. The cortical thickness is also decreased after ovariectomy.

algorithms, free from model assumptions used in 2D histomorphometry, have been developed to segment and directly quantify 3D trabecular bone structure[9,11,19]. Trabecular thickness (Tb.Th) is determined by filling maximal spheres in the structure with the distance transformation. Then the average thickness of all bone voxels is calculated to give Tb.Th.

Trabecular separation (Tb.Sp) is calculated with the same procedure, but the voxels representing nonbone parts are filled with maximal spheres. Tb.Sp is thus the thickness of the marrow cavities. Trabecular number (Tb.N) is taken as the inverse of the mean distance between the mid-axes of the observed structure. The mid-axes of the structure are assessed from the binary 3D image using the 3D distance transformation and extracting the center points of nonredundant spheres which fill the structure completely. Then the mean distance between the mid-axes is determined in analogy to the Tb.Sp calculation, i.e., the separation between the mid-axes is assessed.

The deterioration of trabecular bone structure is characterized by a conversion from plate elements to rod elements. Consequently the terms “rod-like” and “plate-like” are frequently used for a subjective classification of cancellous bone. A new morphometric parameter called structure model index (SMI) is introduced, which makes it possible to quantify the characteristic form of a 3D described structure in terms of the amount of plates and rod composing the structure. The SMI is calculated by means of 3D image analysis based on a differential analysis of the triangulated bone surface.

For an ideal plate and rod structure the SMI value is 0 and 3, respectively, independent of the physical dimensions. For a structure with both plates and rods of equal thickness the value lies between 0 and 3, depending on the volume ratio of rods and plates. The geometrical degree of anisotropy (DA) is defined as the ratio between the maximal and the minimal radius of the mean intercept length (MIL) ellipsoid. The MIL distribution is calculated by superimposing parallel test lines in different directions on the 3D image. The directional MIL is the total length of the test lines in one direction divided by the number of intersections with the bone marrow interface of the test lines in the same direction. The MIL ellipsoid is calculated by fitting the directional MIL to a directed ellipsoid using a least square fit.

While the early implementations of 3D μCT focused more on the technical and methodological aspects of the systems, the recent development emphasized the practical aspects of micro-tomographic imaging. μCT has been used to measure trabecular bone structure in rats. Most studies have focused on the trabecular bone in the proximal tibial metaphysis. Now, increased attention is being focused on the trabecular bone in the rat vertebra, because of its similarity to a human fracture site, and because of the greater ease of performing biomechanical testing[3].

We investigated the 3D trabecular bone structure of the vertebral body in OVX rats treated with estrogen replacement therapy (ERT)[20]. Female rats of 6-month were divided randomly into baseline, sham-OVX, OVX, and OVX treated with estrogen, and observed for 9 months post-OVX. The lumbar vertebrae were harvested, and scanned using a compact fan-bean-type μCT scanner (μCT 20, Scanco Medical AG, Bassersdorf, Switzerland) with isotropic resolution of 11 μm^3. Images are acquired in either spiral scan or multislice mode. A small x-ray tube with a μfocus is used as a source. Its focal spot has a nominal diameter of 10 μm.

The detector consists of a linear CCD-array with 1024 elements with a pitch of 25 μm[18]. Three D trabecular structure was directly measured in the vertebral body excluding the primary spongiosa. BMC and BMD were also determined using a pencil beam DXA (QDR 1000, Hologic, Waltham, MA). Biomechanical testing of the vertebral body was performed using a servo-hydraulic testing machine (MTS Bionix, Minneapolis, MN). The results show that OVX induces significant bone loss in rats (Fig. 1), while ERT prevents OVX-induced changes. μCT 3D trabecular parameters show greater changes than DXA measurement, and show stronger correlation with biomechanical properties.

We studied the anabolic effects of low-dose (5 ppm in drinking water) long-term (9 months) sodium fluoride (NaF) treatment in intact and OVX rats[21]. μCT examination with isotropic resolution of 11 μm^3 showed that there was a statistically significant increase in 3D BV (9%) and Tb.Th (14%) in NaF treated animals compared with non-treated animals.

There was no significant change in Tb.N and Tb.Sp between treated and non-treated animals. There was a significant increase in DXA BMC (5%) and BMD (2%) in NaF treated animals, compared with controls. No significant

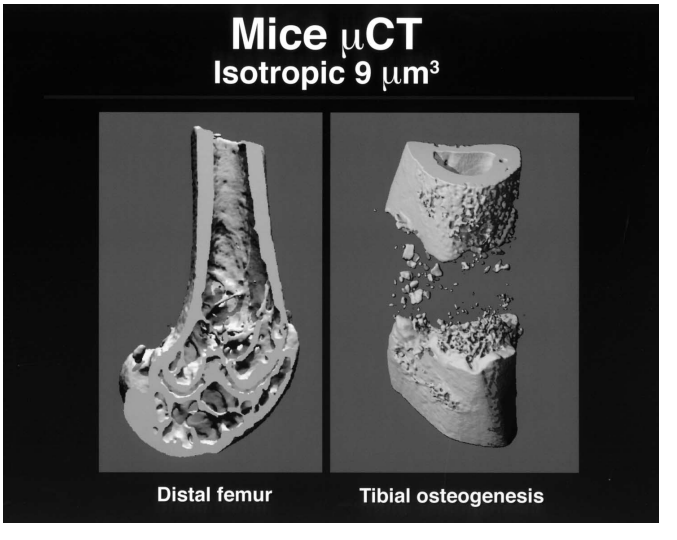

Figure 2. μCT 3D images (isotropic resolution of 9 μm^3) of trabecular and cortical bone structure of a mouse (left), and bone formation in the distraction gap in a mouse model of osteogenesis using Ilizarov leg lengthening procedures (right).

change was found in compressive strength, stiffness, toughness, and deformation between treated and non-treated animals. The data indicated NaF treatment increases Tb.BV in the lumbar vertebral body, possibly by increasing Tb.Th through increasing bone formation on existing trabeculae. However, such increases do not translate into a corresponding increase in bone biomechanical properties. μCT 3D trabecular parameters show greater changes than DXA.

We have demonstrated that 3D μCT can quantify mouse trabecular and cortical bone structure (Fig. 2) with an isotropic resolution of 9 μm^3. It is also useful for studying osteoporosis in mice and in phenotypes of transgenic mice or gene knockout mice. μCT can be used to quantify osteogenesis in mouse Ilizarov leg lengthening procedures, to quantify osteoconduction in a rat cranial defect model (Fig. 3), and to quantify cortical bone porosity.

Synchrotron μCT at 23 μ/voxel in the proximal tibial metaphysis of live rats[22-24] shows that trabecular connectivity decreased 27% by days 5 and 8 post-OVX and continued to decrease up to day 50 post-OVX. The trabecular BV decreased 25% by 8 days post-OVX, and it continued to decrease through day 50. Trabecular bone connectivity and volume deteriorate rapidly while DPD cross-link excretion increased more slowly after OVX. When ERT was delayed 5-13 days post-OVX, declines in BV and connectivity occurred.

ERT restored BV, but not connectivity, to baseline levels by allowing bone formation to continue in previously activated bone remodeling units while suppressing the production of new remodeling units. Intermittent hPTH(1-34) treatment in osteopenic OVX rats increased trabecular BV to control levels or higher by thickening existing trabeculae. Human PTH(1-34) did not re-establish connectivity when therapy was started after 50% of the trabecular connectivity was lost.

μMRI

MRI, a complex technology based on the application of high magnetic fields, transmission of radiofrequency waves and detection of radiofrequency signals from excited hydrogen protons, can clearly delineate trabecular bone. This is because bone mineral lacks free protons and generates no MR signal while adjacent soft tissue and marrow contain abundant free protons and give a strong signal.

Unlike μCT, it is nonionizing. Its assessment of human osteoporosis has been well investigated[7]. The parameters derived from the low-resolution images were found to account for 91% of the variation in Young's modulus, suggesting that noninvasive assessment of the mechanical competence of trabecular bone in osteoporotic patients may be feasible[25].

Recently, the ability of μMRI to assess osteoporosis in animal models has been explored in depth. We have demonstrated that using a small high-efficiency coil in high-field imager, μMRI can provide resolutions sufficient to discriminate individual trabeculae. μMRI of trabecular structure in the distal radius shows trabecular bone loss after OVX, corresponding to the histology of the same rat (Fig. 4). A μMRI of a rat tail shows 3D cortical bone, trabecular network, and other soft tissue. μMRI shows increased bone mass in the distal femoral metaphysis of rats treated with a bisphosphonate, increased cartilage thickness in the growth plate, and corresponding recovery changes after withdrawal of treatment. The trabecular structure in the femoral neck of a ewe can be clearly shown on μMRI[1]. In our study, with

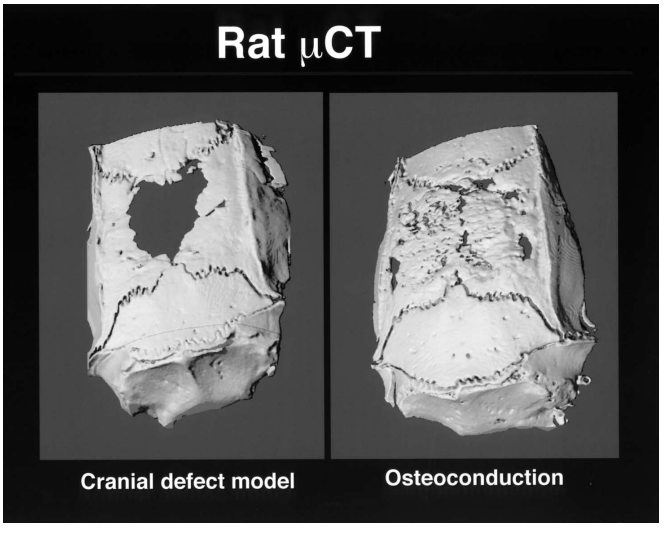

Figure 3. μCT 3D images of rat cranial defect model (left) and its corresponding osteoconduction/osteogenesis in the cranial defect after treatment (right).

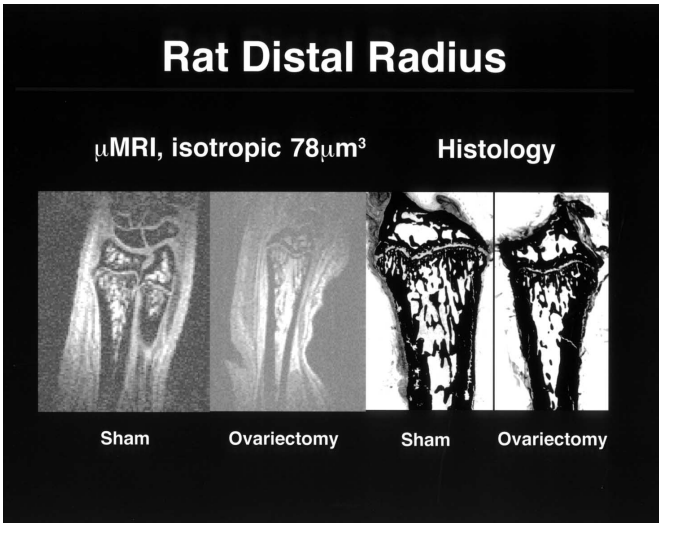

Figure 4. μMRI using a solenoid coil and a 2-Tesla imager (GE/Bruker) with isotropic resolution of 78 μm^3, and their corresponding histology of the distal radius show loss in trabecular structure after ovariectomy in rats.

appropriate choices, it is possible to image trabecular bone in rats in vivo and in vitro. Segmenting trabecular bone from adjacent tissues has been a useful technique in the quantification of trabecular bone in MRI images. In our study of OVX in rats, analysis of μMRI demonstrated differences in rat trabecular bone that are not detected by DXA measurements[26].

μMRI showed OVX induced loss in trabecular BV and structure, which were prevented by ERT[27]. There are excellent correlations between μMRI with resolution up to 24x24x250 μ and histological assessment of intact rat tibiae and vertebrae[28]. Recently, it has been reported that rat tibiae were imaged at 9.4 T in vitro with isotropic resolution of 46 μm^3. It has shown that alendronate maintains trabecular BV and structure about midway between intact and OVX, whereas PGE_2 returned them to intact levels[29].

μMRI shows 3D bone structure, and some other tissues at the same time. In the rabbit's knee, μMRI shows trabecular structure and cartilage. In the OA model induced by meniscectomy[30] or anterior cruciate ligament transection[31], MRI shows subchondral osteosclerosis, and decreased cartilage thickness (Fig. 5). MRI also shows osteophytes in a rabbit OA model. However, radiographs can only show subchondral osteosclerosis, while osteophytes could not be found in a rabbit OA model.

Although high-resolution MR has been used successfully for in vitro quantitative evaluation of human trabecular bone[32], application of this technology to small-animal bone is more demanding, as resolution requirements are more stringent because of the considerably smaller trabecular size. The need for higher resolution, dictated by the thinner trabeculae, entails a significant penalty for signal to noise ratio and acquisition time.

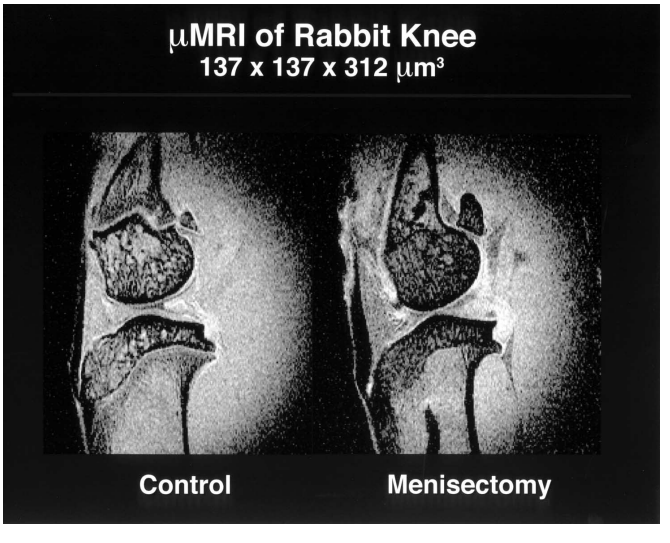

Figure 5. Fat-suppressed 3D gradient-echo images were obtained from knees of adult rabbits, using a Helmholtz coil and a 2-Tesla system (GE/Bruker), imaged in sagittal plane (TR 110/TE 3.5 ms; NEX 2; fat-sat; voxel dimensions 137 μm X 137 μm in-plane X 312 μm thick). The acquisition time was 1 hr. Sagittal slice through the medial chondyle show normal structure of cartilage, menisci, subchondral bone and trabecular bone network in normal control (left); decreased cartilage thickness, osteosclerosis and osteophytes at 3-month post bilateral partial medial menisectomy.

Summary

Advanced imaging methods of bone structure have several advantages, though their equipment and techniques are demanding. They are unbiased methods, are free from the model assumptions used in 2D histomorphometry.

They are able to directly measure 3D structure and connectivity in arbitrary orientations in a highly automated, fast, objective, non-user-specific manner, with little sample preparation, allowing greater numbers of samples for unbiased comparisons between controls and the disordered or treated.

They can have large sample size and therefore less sampling error. They are non-destructive which allows multiple tests such as biomechanical testing and chemical analysis on the same sample, and non-invasive which permits longitudinal studies and reduces the number of animals needed. They require robust image processing algorithms to segment and quantify bone structure, and may have limitations in spatial resolution for certain structures.

They can not provide information on cellular activities and on dynamic mineralization processes. Rather than replacing bone histomorphometry, they may complement to each other in the evaluation of osteoporosis and other bone disorders.

References

1. Jiang Y. Radiology and Histology in the Assessment of Bone Quality. Leuven: Peeters & Jiang, 1995.
2. Wevers M, De Meester P, Lodewijckx M, Ni Y, Marchal G, Jiang Y, Dequeker J, Geusens P, Vandeursen H, De Ridder D, Baert L, Pittomvils G, Boving R. Application of microfocus x-ray radiography in materials and medical research. NDT & E International 1993; 26: 135-140.
3. Jiang Y, Zhao J, Genant HK, Dequeker J, and Geusens P. Long-term changes in bone mineral and bio-mechanical properties of vertebrae and femur in aging, dietary calcium restricted and/or estrogen-deprived/-replaced rats. J Bone Miner Res 1997; 19:820-831.
4. Rosen HN, Tollin S, Balena R, Middlebrooks VL, Beamer WG, Donohue LR, Rosen C, Turner A, Holick M, Greenspan SL. Differentiating between orchiectomized rats and controls using measurements of trabecular bone density: A comparison among DXA, histomorphometry, and peripheral quantitative compu-terized tomography. Calcif Int Tissue 1995; 57:35-39.
5. Jiang Y, Zhao J, Augat P, Ouyang X, Lu Y, Majumdar S, Genant HK. Trabecular bone mineral and calculated structure of human bone specimens scanned by peripheral quantitative computed tomography: Relation to biomechanical properties. J Bone Miner Res

1998; 13:1783-1790.
6. Jiang Y, Zhao J, Rosen C, Geusens P, Genant HK. Perspectives on bone mechanical properties and adaptive response to mechanical challenge. J Clin Densitometry 1999; 4: 423-433.
7. Genant HK, Gordon C, Jiang Y, Lang TF, Link TM, Majumdar S. Advanced imaging of bone macro and micro structure. Bone 1999; 25:149-152.
8. Parfitt AM. The sterologic basis of bone histomorphometry. Theory of quantitative microscopy and reconstruction of the third dimension. In: Recker R (ed) Bone Histomorphometry. Techniques and Interpretations. CRC Press, Boca Raton, FL, 1983:53-87.
9. Hildebrand T, Laib A, Muller R, Dequeker J, Ruegsegger P. Direct three-dimensional morphometric analysis of human cancellous bone: micro-structural data from spine, femur, iliac crest, and calcaneus. J Bone Miner Res 1999; 14:1167-1174.
10. Guilak F. Volume and surface area of viable chondrocytes in situ using geometric modeling of sense confocal sections. J Microsc 1994; 173:245-256.
11. Hildebrand T and Ruegsegger P. A new method for the model independent assessment of thickness in three-dimensional images. J Microsc 1997; 185:67-75.
12. Odgaard A, Gundersen HJG. Quantification of connectivity in cancellous bone, with special emphasis on 3-D reconstruction. Bone 1993; 14:173-182.
13. Feldkamp LA, Goldstein SA, Parfitt AM, Jesioil G, Kleerekoper M. The direct examination of three-dimensional bone architecture in vitro by computed tomography. J Bone Miner Res 1989; 4:3-11.
14. Kinney JH, Lane NE, Haupt DL. In vivo, three-dimensional microscopy of trabecular bone. J Bone Miner Res 1995; 10:264-270.
15. Smith CB, Silver MD. Comparison between single slice CT and volume CT. In: Czichos HCH, Schnitger D (eds.) International Symposium on Computerized Tomography for Industrial Applications, Bundes-ministerium des Innern, Bundesanstalt fur Material-forschung und Prufung, Berlin, Germany, 8-10 June, 1994.
16. Bonse U, Busch F, Gunnewig 0, Beckmann F, Pahl R, Delling G, Hahn M, Graeff W. 3D computed X-ray tomography of human cancellous bone at 8 μm spatial and 10-4 energy resolution. Bone Miner 1994; 25:25-38.
17. Peyrin F, Salome M, Cloetens P, Ludwig W, Ritman, Ruegsegger P, Laval-Jeantet AM and Baruchel J. What do micro-CT examinations reveal at various resolutions: a study of the same trabecular bone samples at the 14, 7, and 2 micron level. Presented, Symposium on Bone Architecture and the Competence of Bone. Ittingen, Switzerland 3-5, 1998.
18. Ruegsegger P, Koller B, Muller R. A microtomographic system for the nondestructive evaluation of bone architecture. Calcif Tissue Int 1996; 58:24-29.
19. Hildebrand T, Ruegsegger P. Quantification of bone microarchitecture with the structure model index. Comp Meth Biomech Biomed Eng. 1997a; 1:15-23.
20. Jiang Y, Zhao J, Prevrhal S, Genant HK. Three-dimensional trabecular microstructure, bone mineral density, and biomechanical properties of the vertebral body of ovariectomized rats with estrogen replacement therapy. J Bone Miner Res 1999; 14(S1):S534.
21. Zhao J, Jiang Y, Prevrhal S, Genant HK. Effects of low dose long-term sodium fluoride on three-dimensional trabecular microstructure, bone mineral, and biomechanical properties of rat vertebral body. The VIIIth Congress of the International Society of Bone Morphometry, Scottsdale, Arizona, 1999: 22.
22. Lane NE, Thompson JM, Strewler GJ, Kinney JH. Intermittent treatment with human parathyroid hormone (hPTH[1-34]) increased trabecular bone volume but not connectivity in osteopenic rats. J Bone Miner Res 1995;10:1470-1477.
23. Lane NE, Thompson JM, Haupt D, Kimmel DB, Modin G, Kinney JH. Acute changes in trabecular bone connectivity and osteoclast activity in the ovariectomized rat in vivo. J Bone Miner Res 1998;13:229-236.
24. Lane NE, Haupt D, Kimmel DB, Modin G, Kinney JH. Early estrogen replacement therapy reverses the rapid loss of trabecular bone volume and prevents further deterioration of connectivity in the rat. J Bone Miner Res 1999; 14:206-214.
25. Hwang SN, Wehrli FW, Williams JL. Probability-based structural parameters from 3D NMR images as predictors of trabecular bone strength. Med Physics 1997; 24:1255-1261.
26. White D, Schmidlin O, Jiang Y, Zhao J, Majumdar S, Genant H, Sebastian A, Morris Jr RC. MRI of trabecular bone in an ovariectomized rat model of osteoporosis. Proceeding of the International Society for Magnetic Resonance in Medicine 5th Scientific Meeting and Exhibition, Vancouver, B.C., Canada. 1997; 2:1021.
27. Kapadia RD, Stroup GB, Badger AM, Koller B, Levin JM, Coatney RW, Dodds RA, Liang X, Lark MW, Gowen M. Applications of micro-CT and MR microscopy to study pre-clinical models of osteoporosis and osteoarthritis. Technol Health Care 1998; 6:361-372.
28. Kapadia RD, High WB, Soulleveld HA, Bertolini D, Sarkar SK. Magnetic resonance microscopy in rat skeletal research. Magn Reson Med 1993; 30:247-250.
29. Takahashi M, Wehrli FW, Wehrli SL, Hwang SN, Lundy MW, Hartke J, Borah B. Effect of prostaglandin and bisphosphonate on cancellous bone volume and structure in the ovariectomized rat studied by quantitative three-dimensional nuclear magnetic resonance microscopy. J Bone Miner Res 1999; 14:680-689.
30. Jiang Y, White D, Zhao J, Peterfy C, Genant HK. Meniscectomy-induced osteoarthritis model in rabbits: MRI and radiographic assessments. Arthritis Rheum 1997; 40(9):S89.
31. Zhao J, Jiang Y, White DL, Han B, Genant HK. Osteoarthritis model in rabbits induced by anterior

cruciate ligament transection: MRI, radiographic, and histologic assessments. Arthritis Rheum 1999; 42:S259.
32. Majumdar S, Genant HK, Grampp S, Newitt DC, Truong VH, Lin JC, Mathur A. Correlation of trabecular bone structure with age, bone mineral density, and osteoporotic status: In vivo studies in the distal radius using high resolution magnetic resonance imaging. J Bone Miner Res 1997; 12:111-118.